A two-layer control architecture for operational management and hydroelectricity production maximization in inland waterways using model predictive control

Karimi Pour, Fatemeh; Segovia Castillo, P.; Duviella, Eric; Puig, Vicenç

DOI
10.1016/j.conengprac.2022.105172

Publication date
2022

Document Version
Final published version

Published in
Control Engineering Practice

Control Engineering Practice 124 (2022) 105172

Contents lists available at ScienceDirect

Control Engineering Practice

journal homepage: www.elsevier.com/locate/conengprac

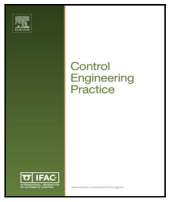

A two-layer control architecture for operational management and hydroelectricity production maximization in inland waterways using model predictive control

Fatemeh Karimi Pour [a,*], Pablo Segovia [b], Eric Duviella [a], Vicenç Puig [c]

[a] IMT Nord Europe, Institut Mines-Télécom, Centre for Digital Systems, F-59000 Lille, France
[b] Department of Maritime and Transport Technology, Delft University of Technology, Delft, The Netherlands
[c] Advanced Control Systems Group, Universitat Politècnica de Catalunya, Institut de Robòtica i Informàtica Industrial (CSIC-UPC), c/ Llorens i Artigas 4-6, 08028 Barcelona, Spain

ARTICLE INFO

Keywords:
Inland waterways
Hydroelectricity generation
Multi-layer architecture
Model predictive control
Moving horizon estimation

ABSTRACT

This work presents the design of a combined control and state estimation approach to simultaneously maintain optimal water levels and maximize hydroelectricity generation in inland waterways using gates and ON/OFF pumps. The latter objective can be achieved by installing turbines within canal locks, which harness the energy generated during lock filling and draining operations. Hence, the two objectives are antagonistic in nature, as energy generation maximization results from optimizing the number of lock operations, which in turn causes unbalanced upstream and downstream water levels. To overcome this problem, a two-layer control architecture is proposed. The upper layer receives external information regarding the current tidal period, and determines control actions that maintain optimal navigation conditions and maximize energy production using model predictive control (MPC) and moving horizon estimation (MHE). This information is provided to the lower layer, in which a scheduling problem is solved to determine the activation instants of the pumps that minimize the error with respect to the optimal pumping references. The strategy is applied to a realistic case study, using a section of the inland waterways in northern France, which allows to showcase its efficacy.

1. Introduction

The environmental, economic and societal effects induced by real-time control and administration of inland waterways make it a domain of increased concern. These are large-scale systems constituted by interconnected real rivers and man-made ducts, and are principally used to freight goods and passengers. Inland waterways are divided into reaches, i.e., parts of a water flow among two hydraulic constructions such as locks and gates, to facilitate their study. More often than not, reaches are characterized by negligible slopes, hence the backwater effect (back-and-forth mass transport phenomenon) becomes of increasing importance. On the other hand, dynamics of inland waterways are relatively slow, which leads to long time delays in the system. These two distinctive aspects complicate the management of these systems.

Inland waterways are dynamic systems which can be characterized via the aggregation of various elements and subsystems, e.g., lock operations, actuators, nodes and reaches. The major operational goal is that of guaranteeing navigability, i.e., ensure that water levels are such that vessels can sail without danger (Rajaoarisoa, Horvath, Duviella, & Chuquet, 2014). In fact, a setpoint known as the normal navigation level (NNL) is defined for each reach. Then, the goal consists in steering the water levels to the designated setpoints. Besides, the navigation rectangle is determined by means of higher and lower navigation levels (HNL and LNL, respectively), which surround the NNL and define the water level bounds. Therefore, the navigability condition can be guaranteed provided that the levels are preserved within the bounds. Furthermore, optimal inland waterways control is tasked with ensuring the navigability condition while fulfilling additional goals, such as minimizing operational costs and extending useful life of the equipment.

Another issue that should be considered is the fact that inland waterways are connected to the sea to eliminate the excess of water in the network. Gates and pumping stations (PS) situated at the outlet of the last reach are used for this purpose. However, sea tides generally restrict the use of these gates for safety reasons, and thus their use is generally prohibited during high tide periods. This situation leads to a hybrid operating situation, one mode for low tide and another for high tide. Therefore, two different operational modes must be considered.

All these features render inland waterways rather challenging to regulate, and advanced control methods are required to achieve the objectives (Litrico, Malaterre, Baume, & Ribot-Bruno, 2008). One of the

* Corresponding author.
E-mail address: fatemeh.karimi-pour@imt-nord-europe.fr (F. Karimi Pour).

https://doi.org/10.1016/j.conengprac.2022.105172
Received 22 September 2021; Received in revised form 29 January 2022; Accepted 31 March 2022
Available online xxxx
0967-0661/

most prominent advanced control strategies, and which has found much success in water systems management, is model predictive control (MPC). Broadly speaking, the sequence of control actions is determined as the solution of an optimization-based control problem that allows to achieve the operational objectives and complies with the set of restrictions, linked to physical/operational conditions and the system model (Karimi Pour, Puig, & Ocampo-Martinez, 2017). Consequently, MPC offers an appropriate framework to fulfil operational management of water systems, because it enables calculation of optimal control actions ahead of time. As an illustration of its applicability, MPC was used in Van Overloop, Negenborn, De Schutter and Van De Giesen (2010) to ensure navigable water levels, provide water resources during dry times and protect against overflows and sea tides. The combined navigability of river systems and water supply were undertaken by applying MPC in Puig, Ocampo-Martínez, and Negenborn (2015). In Nguyen, Prodan, Lefevre, and Genon-Catalot (2017), several non-centralized MPC approaches were tested on irrigation canals and their performances were compared. The link between the reliability of sewer systems and water supply was studied employing MPC in Karimi Pour, Puig, and Cembrano (2020). An economic MPC was designed in Karimi Pour, Puig, and Cembrano (2019b) to minimize the economic costs incorporated with water processing and pumping for water distribution networks.

It must be noted that MPC requires knowledge of the system states at each time instant. Since the state vector is seldom completely measurable, the use of an observer that estimates this information and provides it to the MPC is required. Even though there exist many state estimation techniques, moving horizon estimation (MHE) is employed in this work. This approach is regarded as the counterpart of MPC, and combining MPC and MHE is indeed interesting, as the MHE is cast as an online optimization problem that can deal with restrictions (Copp & Hespanha, 2017). The combined MPC-MHE approach has been used in different frameworks such as unmanned aerial vehicles (Quintero, Copp, & Hespanha, 2015), autonomous agricultural vehicles (Kraus et al., 2013), airborne wind energy systems (Vukov et al., 2015) and preventive sensor maintenance (Lao, Ellis, Durand, & Christofides, 2015). However, this combination has not been widely applied to water systems in general and navigation canals in particular. In Breckpot, Blanco, and De Moor (2010), MPC-MHE is used for flood prevention purposes, and its implementation is evaluated through a three-position controller. In Joseph-Duran, Ocampo-Martinez, and Cembrano (2015), pollution mitigation for sewer networks based on the output-feedback control approach is investigated. In Segovia, Rajaoarisoa, Nejjari, Duviella, and Puig (2019), an MPC-MHE is designed to regulate water levels in inland waterways.

On a separate note, the last few decades have witnessed an energy crisis, mainly caused by the depletion of fossil fuel energy sources. This has been a major motivator factor for researchers to look into renewable energy sources. Design and control of systems that can utilize wind or tidal energy have been widely studied, and the aim is similar to the problem of converting canal lock hydroelectric power plant to electrical energy (Yin et al., 2016; Zhang et al., 2017; Zhou, Scuiller, Charpentier, Benbouzid, & Tang, 2013). Over the last years, several studies have aimed at improving the capability of machines to produce energy from low and very low water sources for various applications such as irrigation canals and river dams. In standard hydropower systems, the manager controls the rotation speed of the turbine to generate energy. In contrast, the case under study considers an immersed turbine inside the lock, whose blades rotate as a result of the water flow. Indeed, the hydraulic turbine is placed inside of a canal lock, and harnesses hydraulic energy to generate electricity. This configuration has already been discussed in Desy and Virta (2005).

A significant advantage of hydroelectricity over wind and photovoltaic energy sources is that the latter are completely weather-dependent, while canal lock hydropower is predictable. Moreover, and taking into account that the flow rate changes according to lock and canal sizes, the energy variation for a particular turbine can be anticipated. For instance, in the *Hauts-de-France* region, there are over 200 canal locks that allow containers and products to be transported. Therefore, feeding turbines (which in turn generate hydroelectricity) using the power generated during lock operations could alleviate the dependency on non-renewable energy sources. Several examples of this can be found in the literature, such as power production optimization for cascaded hydropower plants (Ribeiro, Guedes, Smirnov, & Vilela, 2012), and the use of MPC to control the turbine discharge of river power plants while complying with constraints: navigational and economical (Setz, Heinrich, Rostalski, Papafotiou, & Morari, 2008), and dictated by authorities (Şahin & Morari, 2010). Furthermore, actual accomplishments of predictive controllers for hydropower production are dealt with in Ackermann et al. (1997) and Maestre et al. (2015). However, no approach has been found which considers simultaneous energy production maximization by increasing the lock operation using an MPC, and regulating water levels in inland waterways. Moreover, the fact that inland waterways are connected to the sea and are thus affected by tides constitutes an additional difficulty at the control design stage.

The main contribution of this paper is design of an improved two-layer control and state estimation strategy. Previous results were presented in Segovia, Duviella, and Puig (2020) and Guekam, Segovia, Etienne, and Duviella (2021), which tackled single and multiple canals (with different objective prioritization), respectively. However, the focus was exclusively put on the water level regulation problem. Conversely, this work considers the additional issue of hydroelectricity generation. This objective can be achieved by means of hydraulic turbines installed inside canal locks to harness hydraulic energy generated during lock filling and draining operations. Therefore, the number of lock operations should be increased to maximize hydroelectricity generation. However, each lock operation leads to unbalanced water levels at the upstream and downstream canals of the lock. It is crucial that hydroelectricity generation is not achieved at the expense of causing the levels to be outside the navigation rectangle. The proposed two-layer approach is designed to simultaneously guarantee system navigability and maximize energy generation, while also taking into account other issues such as control effort and equipment deterioration. Furthermore, the proposed strategy is applied to a realistic model of part of the inland waterways in northern France, and is tested by means of an advanced hydraulic software tool that allows to accurately reproduce the behaviour of the real system.

The paper is structured as follows. The general inland waterways description and its control-oriented model are presented in Section 2. The control problem and operational objectives are outlined in Section 3. Then, the proposed two-layer is detailed in Section 4. Case study description and discussion of results, which allows to validate the efficiency of the proposed method, are included in Section 5. Lastly, conclusions are illustrated and the next steps are outlined in Section 6.

Notation

Throughout this paper, let $\mathbb{R}$, $\mathbb{R}^n$, $\mathbb{R}^{m\times n}$ and $\mathbb{Z}_{\geq 0}$, denote the field of real numbers, the set of column real vectors of length n, the set of m by n real matrices and the set of non-negative integers, respectively. Moreover, $\|\cdot\|$ denotes the spectral norm for matrices, all vectors are column vectors unless otherwise stated, 0 indicates zero column vector of appropriate dimensions and I_δ denotes the identity matrix of dimension δ. The superscript ^{T} represents the transpose, and operators $<, \leq, =, >, \geq$ denote element-wise relations of vectors.

2. System description and control-oriented modelling

Different modelling methods for inland waterways are presented in the literature (see, e.g., Horváth et al. (2014), Karimi, Puig and Ocampo-Martinez (2019), Segovia et al. (2018), Van Overloop et al.

(2010) and Weyer (2001)). An inland waterways model might be conceived as a set of fundamental components: actuators, lock operations, nodes and reaches, each characterized by means of different relations. Moreover, the physical nature of certain variables, e.g., flows, openings, elevations and water levels, and other factors in the waterways constrain the evolution of the system dynamics.

2.1. Gates and pumps

Water levels in inland waterways can be adjusted using gates. While several variables can be used as manipulated inputs, e.g., openings, elevations and flows (Horváth, Galvis, Gómez, & Rodellar, 2015a), discharge is considered as the control variable in this work. These components have upper and lower operating bounds

$$\underline{u}^g \leq u^g(k) \leq \overline{u}^g, \qquad g = 1, \dots, N_g, \tag{1}$$

where $\overline{u}^g$ and $\underline{u}^g$ are the upper and lower boundary of the gth gate, and N_g is the total number of gates in the system.

Moreover, pumps installed in pumping stations are considered to be fixed-speed pumps (FSP) due to their simpleness, i.e., they can be used in an ON/OFF manner. This behaviour usually prevents the equipment from satisfying the exact optimal reference. Pump flows are thus the manipulated variables subject to physical limits, which can be expressed as

$$\underline{u}^p \leq u^p(k) \leq \overline{u}^p, \qquad p = 1, \dots, M_p, \tag{2}$$

where $\overline{u}^p$ and $\underline{u}^p$ are the upper and lower bounds of the pth pump, and M_p denotes the number of the pumps in the system.

2.2. Lock operations

Navigation from one reach to another is achieved through locks, which are enclosures that allow vessels to cope with the different elevation of the reaches. Lock operation demand, which is considered as a system disturbance and denoted by d_k, makes it more challenging to maintain the levels near the setpoints. Despite the fact that lock operations cannot be exactly predicted or delayed for a long time, it is possible to slightly anticipate them. Whenever a vessel crosses a lock, its director notifies the other lock managers. Then, by considering the distance between locks and the average vessel speed, its arrival time to the upcoming locks can be predicted, with an error of a few minutes, thus allowing for lock operation time-series predictions ahead of time.

2.3. Turbines

During lock chamber filling and draining operations, the water level inside the lock reaches similar levels as the downstream or upstream reach. Afterwards, the ship is able to move inside the lock. Thus, installing hydraulic turbines inside canal locks allows to recover the unused hydraulic energy, and thus produce electricity. Some of these lock operations can be requested by the turbines. Then, the disturbances related to the specific lock that contains the turbine are denoted by $d^{lo} \in d$. According to Leontidis et al. (2016), knowledge regarding time and characteristics of the lock operation makes it possible to estimate the average energy produced during each lock operation. In this paper, specifications of the turbines and the characteristics of lock operations are considered as in Leontidis et al. (2016).

2.4. Reaches

A detailed description of inland waterways is required at the control design step to calculate the predicted value at future time intervals. In this regard, the Saint-Venant nonlinear partial differential equations (Chow, 1959) represent the most precise model. However, their excessive sensitivity to geometric errors and uncaptured phenomena do not make them well suited for control. A simpler solution consists in performing linearization of the Saint-Venant equations to obtain a linear model around an operating point. For instance, Integrator Delay (ID) model (Schuurmans, Clemmens, Dijkstra, Hof, & Brouwer, 1999), Integrator Resonance (IR) model (Van Overloop, Miltenburg et al., 2010), Integrator Delay Zero (IDZ) model (Litrico & Fromion, 2009), black-box (Weyer, 2001) and grey-box (Horváth et al., 2014) models.

In this work, the IDZ model is selected. This input–output model establishes a relationship between the water levels and discharges at the boundaries of a single reach (portion of the water course bounded between two hydraulic structures) as follows:

$$\begin{bmatrix} h_1(s) \\ h_2(s) \end{bmatrix} = \begin{bmatrix} p_{11}(s) & p_{12}(s) \\ p_{21}(s) & p_{22}(s) \end{bmatrix} \begin{bmatrix} q_1(s) \\ q_2(s) \end{bmatrix}, \tag{3}$$

where $h_1(s)$ and $h_2(s)$ denote the upstream and downstream water levels, $q_1(s)$ and $q_2(s)$ define the upstream inflow and downstream outflow, and $p_{ij}(s)$ represent the IDZ expressions.

A discrete-time linear state–space representation of the IDZ model (3) can be formulated following the derivation in Segovia et al. (2019), and is given by

$$\begin{aligned} x(k+1) = {} & \begin{bmatrix} 1 & 0 \\ 0 & 1 \end{bmatrix} x(k) + \begin{bmatrix} T_s & 0 \\ 0 & -T_s \end{bmatrix} \left(u^g(k) + u^p(k) \right) \\ & + \begin{bmatrix} 0 & -T_s \\ T_s & 0 \end{bmatrix} \left(u^g(k-\tau) + u^p(k-\tau) \right), \end{aligned} \tag{4a}$$

$$\begin{aligned} y(k) = {} & \begin{bmatrix} \frac{1}{A_u} & 0 \\ 0 & \frac{1}{A_d} \end{bmatrix} x(k) + \begin{bmatrix} \frac{z_{11}}{A_u} & 0 \\ 0 & -\frac{z_{22}}{A_d} \end{bmatrix} \left(u^g(k) + u^p(k) \right) \\ & + \begin{bmatrix} 0 & -\frac{z_{12}}{A_u} \\ \frac{z_{21}}{A_d} & 0 \end{bmatrix} \left(u^g(k-\tau) + u^p(k-\tau) \right), \end{aligned} \tag{4b}$$

where $x(k) \in \mathbb{R}^{n_x}$ denotes the water volumes, $u^g(k) \in \mathbb{R}^{n_{ug}}$ and $u^p(k) \in \mathbb{R}^{n_{up}}$ are the manipulated gate and pumping actions introduced in Section 2.1, and $y(k) \in \mathbb{R}^{n_y}$ are the water levels. Moreover, T_s is the sampling time, τ is the delay of the reach (in samples), and A_u, A_d, z_{11}, z_{12}, z_{21} and z_{22} are parameters of the p_{ij} expressions in (3) as shown in Litrico and Fromion (2009).

Remark 1. The relationship between h and q in (3), and y and u^p/u^g in (4) is as follows. On the one hand, h denotes all water levels at the upstream and downstream boundaries of all reaches, while y represents the subset of water levels h that can be measured using water level sensors. On the other hand, q are the physical inflows and outflows at the boundaries of all reaches, while u^p and u^g denote the controlled discharges supplied by the pumps and gates, respectively. □

Navigability imposes constraints on the water levels, although these could be eased for a short period to account for factors like the weather. Such constraints are then relaxed by means of a relaxation parameter α_k, and a quadratic penalty is set on this parameter. Therefore, navigability condition can be given as

$$\underline{y}_{ref} - \alpha(k) \leq y(k) \leq \overline{y}_{ref} + \alpha(k), \tag{5}$$

where $\overline{y}_{ref}$ and $\underline{y}_{ref}$ are the HNL and LNL, respectively. Furthermore, $\alpha(k) \geq 0$.

2.5. Nodes

Inland waterways are characterized by inflows and outflows along the canals. The positions in which these take place are referred to as nodes. These mass balance relations, which represent the static part of the system, can be modelled as equality constraints of the form

$$0 = E_u^g u^g(k) + E_{u\tau}^g u^g(k-\tau) + E_u^p u^p(k) + E_{u\tau}^p u^p(k-\tau) + E_d d(k) + E_{d\tau} d(k-\tau), \tag{6}$$

where all matrices are time-invariant and of suitable dimensions.

2.6. Control-oriented model

The general model formulation is characterized by variables with instantaneous and delayed effects. At each time instant, the control and state estimation problems optimize the values of the variables with an immediate effect, using delayed information (which was computed in previous iterations but whose effect is present at the current time instant) as input parameters to the problems.

The final control-oriented model is built by taking into account the set of compositional elements and the modelling methodology of each component, which have been described in the previous sections . The final model, which describes the dynamics of an inland waterway consisting of multiple reaches, is then characterized by the following set of linear discrete-time equations for all time instants $k \in \mathbb{Z}_+$:

$$\begin{aligned} x(k+1) &= Ax(k) + B_u^g u^g(k) + B_{u\tau}^g u^g(k-\tau) + B_u^p u^p(k) + B_{u\tau}^p u^p(k-\tau) \\ &\quad + B_d d_k + B_{d\tau} d(k-\tau), \end{aligned} \tag{7a}$$

$$\begin{aligned} y(k) &= Cx(k) + D_u^g u^g(k) + D_{u\tau}^g u^g(k-\tau) + D_u^p u^p(k) + D_{u\tau}^p u^p(k-\tau) \\ &\quad + D_d d_k + D_{d\tau} d(k-\tau), \end{aligned} \tag{7b}$$

$$\begin{aligned} 0 &= E_u^g u^g(k) + E_{u\tau}^g u^g(k-\tau) + E_u^p u^p(k) + E_{u\tau}^p u^p(k-\tau) \\ &\quad + E_d d(k) + E_{d\tau} d(k-\tau), \end{aligned} \tag{7c}$$

where $x(k) \in \mathbb{R}^{n_x}$, $u(k) \in \mathbb{R}^{n_u}$ and $y(k) \in \mathbb{R}^{n_y}$ are as in (4), and $d(k) \in \mathbb{R}^{n_m}$ represents the operation of locks (whose effect is that of additive disturbances) as described in Section 2.2. These lock operations are closely linked to the hydroelectricity that can be generated by the turbines, which is detailed in Section 2.3. Moreover, (7a) and (7b) represent the multi-reach versions of (4a) and (4b), respectively, and (7c) represents the mass balances introduced in (6). Furthermore, A, A_τ, B_u, $B_{u\tau}$, B_d, $B_{d\tau}$, C, C_τ, D_u, $D_{u\tau}$, D_d, $D_{d\tau}$, E_u^g, $E_{u\tau}^g$, E_u^p, $E_{u\tau}^p$, E_d and $E_{d\tau}$ are time-invariant matrices of appropriate dimensions, which can be obtained by appropriately combining matrices of individual reaches, given in (4), according to the network topology.

Model (7) describes a particular system characterized by a single time delay τ. The general multi-delay case, where delays can be characterized by the set $S = \{\tau_1, \tau_2, \dots, \tau_r\}$, can be modelled as

$$\begin{aligned} x(k+1) &= Ax(k) + B_u^g u^g(k) + B_u^p u^p(k) + B_d d(k) \\ &\quad + \sum_{\tau_i \in S} \left(B_{u\tau_i}^g u^g(k-\tau_i) + B_{u\tau_i}^p u^p(k-\tau_i) + B_{d\tau_i} d(k-\tau_i) \right), \end{aligned} \tag{8a}$$

$$\begin{aligned} y(k) &= Cx(k) + D_u^g u^g(k) + D_u^p u^p(k) + D_d d(k) \\ &\quad + \sum_{\tau_i \in S} \left(D_{u\tau_i}^g u^g(k-\tau_i) + D_{u\tau_i}^p u^p(k-\tau_i) + D_{d\tau_i} d(k-\tau_i) \right), \end{aligned} \tag{8b}$$

$$\begin{aligned} 0 &= E_u^g u^g(k) + E_u^p u^p(k) + E_d d(k) \\ &\quad + \sum_{\tau_i \in S} \left(E_{u\tau}^g u^g(k-\tau) + E_{u\tau}^p u^p(k-\tau) + E_{d\tau} d(k-\tau) \right). \end{aligned} \tag{8c}$$

3. Problem statement

The primary goal of inland waterways management is to ensure that freight and passengers transport can be carried out in a safe way, which can be achieved by operating cross structures to regulate the levels. However, seamless transport chains are only possible if the water levels are maintained inside the navigation rectangle. Furthermore, the current climate change context requires to minimize water resources misuse.

Canals are managed to convey the water excess to the sea as in the scenarios considered in the case study of this work. To this end, gates and pumping stations are set up at the end of the downstream canal. However, it must be noted that such gates cannot generally be operated during high tide due to safety issues, hence sea tides need to be taken into account. Therefore, two different operating modes (low and high tide) can be distinguished, each of them requiring the design of a different controller. These compute an optimal set of control signals, which in turn should be provided to the local controllers at the cross structures. Such local (or low-level) control is in charge of injecting the optimal reference values, or as close to these as possible. However, while it could be assumed for gates to be able to provide the exact required flow, the same cannot be said about pumping stations. Indeed, they usually consist in a set of ON/OFF pumps, which regularly prevents the equipment from satisfying the exact reference. Then, a possible solution consists in solving the low-level pumping control problem as a scheduling problem. Its solution yields the activation instants of the pumps so that their total effect is as close to the optimal control reference as possible.

An additional operational objective that can be achieved in parallel with level regulation is that of harnessing the energy generated during lock operations. As mentioned before, according to the lock operation procedure, installing a hydraulic turbine inside a canal lock makes it possible to recover the useable hydraulic energy to generate electricity. Utilizing the power generated along the working time of the lock in the available canal equipment is invaluable. This energy is considered as a further advantage derived from lock operation. However, it must be noted that each operation leads to unbalanced upstream and downstream levels, as water is extracted from one reach and transferred to another.

The aforementioned operational objectives can be attained by solving a multi-objective control problem. MPC is an appropriate control approach for inland waterways management, as it is solved as an online optimization problem and its design framework is simple yet powerful. Its main principle consists in calculating an input sequence that steers the predicted system response to the setpoints optimally while respecting the constraints (Karimi Pour, Puig, & Cembrano, 2019a). Then, the set of operational objectives can be achieved by minimizing a multi-objective cost function that can be established as the weighted aggregate of different terms, each related to a particular objective. The following objectives can be considered:

- Keep water levels near the setpoints: the key inland waterways management objective is to maintain the levels near the setpoints, whose mathematical expression is

$$\ell^y(k) \triangleq (y(k) - y_{ref})^\top W_y (y(k) - y_{ref}), \tag{9}$$

  where y_{ref} is the vector of NNL values and W_y defines the weight associated to such objective.
- Maximize energy production: this can be achieved by increasing the number of lock operations (intensifying the number of filling and draining operations) in the reaches. However, and according to operational guidelines, there is a maximum number of lock operations that can be performed. Then, the goal consists in minimizing the difference between the actual and the maximum number of lock operations. Bearing in mind that these lock operations are introduced as a part of system disturbances (Section 2.3), this objective can be formulated as

$$\ell^{ep}(k) \triangleq \left(\overline{d}^{lo} - d^{lo}(k) \right)^\top W_{ep} \left(\overline{d}^{lo} - d^{lo}(k) \right), \tag{10}$$

  where W_{ep} is a diagonal positive definite matrix and $\overline{d}^{lo}$ is the upper bound on the allowed number of lock operations. Moreover, the constraint $\underline{d}^{lo} \leq d^{lo}(k) \leq \overline{d}^{lo}$ must be incorporated into the problem, where $\underline{d}^{lo}$ is the corresponding lower bound.
- Minimize equipment operational cost: this term refers to the economic costs associated to the operation of gates and pumps, which can be expressed as

$$\ell^e(k) \triangleq u(k)^\top W_e u(k), \tag{11}$$

  where W_e is a diagonal positive definite matrix.
- Ensure smooth control actions: the optimal control actions must be smooth to increase the lifespan of the equipment. Thus, the

rate of the control signal among two sequential time instants is optimized as

$$\ell^{\Delta u}(k) \triangleq \Delta u(k)^{\top} W_{\Delta u} \Delta u(k), \tag{12}$$

where $\Delta u(k) \triangleq u(k) - u(k-1)$, and $W_{\Delta u}$ is a diagonal positive definite matrix.

- Penalize relaxation of navigability condition: penalty on α_k, which was presented in (5) to guarantee that the levels are outside the navigation bounds for a minimal amount of time, is defined as

$$\ell^{\alpha}(k) \triangleq \alpha^{\top}(k) W_{\alpha} \alpha(k), \tag{13}$$

where W_{α} is a diagonal positive definite matrix.

Therefore, simultaneous achievement of the different objectives for several canals at the same time can be attained by considering the multi-objective function J, which can be represented as

$$J = \sum_{k=1}^{N_p} \sum_{r=0}^{N_r} \left(\ell^{y,r}(k) + \ell^{e,r}(k) + \ell^{\Delta u,r}(k) + \ell^{\alpha,r}(k) + \ell^{ep,r}(k) \right), \tag{14}$$

where N_r indicates the total number of reaches and N_p is the prediction horizon.

With all this in mind, the control strategy (including the energy management) is defined using a multi-layer architecture, and is conceptualized in two different layers:

- The *upper layer* is provided with the current tidal period by an external source, and solves the appropriate MPC. The solution is a set optimal control setpoints for gates and pumps, which maintain optimal navigation conditions and maximize energy production. Moreover, an MHE is solved to estimate the future state of the system.
- The *lower layer* receives optimal control setpoints for the pumps (gates are assumed to be able to realize the optimal setpoints). A pumping scheduling problem is then solved, which yields the activation instants of the pumps that minimize the error with respect to the optimal control references provided by the upper layer.

4. Proposed approach

4.1. Upper layer

The upper layer is concerned with the MPC and MHE design. The effect of sea tides on system operation is such that gates cannot be utilized during high tides due to safety concerns. Thus, two different operating modes (low and high tide) must be defined. Updated tidal information is provided by an external source at regular time instants. An MPC must be designed for each tidal mode, and the appropriate controller must be selected at every computation time step. On the other hand, the same MHE can be used for both tidal periods, as its purpose is that of performing state estimation according to given input–output data.

The controller structure design follows the ideas presented in Guekam et al. (2021), a modification from Segovia et al. (2020) that allows to consider the case of N_r reaches with different delays $\{\tau_1, \tau_2, \dots, \tau_{N_r}\}$, where τ_r is the delay (in samples) related to the rth reach and $\tau = \max(\tau_r)$, $r \in \{1, \dots, N_r\}$. However, the formulation is further extended in this paper to consider an additional operational objective, i.e., maximize energy generated by the lock turbine as a result of increasing the number of lock operations.

4.1.1. MPC formulation

The multi-objective function (14), physical constraints (1) and (5) and the control-oriented model (8) are gathered to formulate the MPC. The cost function is minimized by solving the optimization-based control problem along the prediction horizon (Karimi Pour, Puig, & Ocampo-Martinez, 2021). The receding-horizon strategy is such that the first value of the control input sequence (MPC solution) is applied to the system, and the rest are neglected. The MPC is then solved at the next time instant by utilizing updated information.

Taking into account that the gates are only used in low-tide mode, the low-tide optimal control actions can be determined as the solution of the following finite-time horizon optimization problem:

$$\min_{\mathbf{u}^p(k), \mathbf{u}^g(k), \mathbf{d}^{lo}(k) \mathbf{y}(k), \boldsymbol{\alpha}(k)} \sum_{i=k}^{k+N_p-1} \left(\ell^{y}(i|k) + \ell^{e}(i|k) + \ell^{\Delta u}(i|k) + \ell^{\alpha}(i|k) - \ell^{ep}(i|k) \right), \tag{15a}$$

subject to:

$$x(i+1|k) = Ax(i|k) + B_u^g u^g(i|k) + B_u^p u^p(i|k) + B_d d(i|k) + \sum_{r=1}^{N_r} S_r \left(B_{u\tau}^g u^g(i-\tau_r|k) + B_{u\tau}^p u^p(i-\tau_r|k) + B_{d\tau} d(i-\tau_r|k) \right), \quad i \in \{k, \dots, k+N_p-1\}, \tag{15b}$$

$$y(i|k) = Cx(i|k) + D_u^g u^g(i|k) + D_u^p u^p(i|k) + D_d d(i|k) + \sum_{r=1}^{N_r} S_r \left(D_{u\tau}^g u^g(i-\tau_r|k) + D_{u\tau}^p u^p(i-\tau_r|k) + D_{d\tau} d(i-\tau_r|k) \right), \quad i \in \{k, \dots, k+N_p-1\}, \tag{15c}$$

$$0 = E_u^g u^g(i|k) + E_u^p u^p(i|k) + E_d d(i|k) + \sum_{\tau_i \in S} \left(E_{u\tau}^g u^g(i-\tau|k) + E_{u\tau}^p u^p(i-\tau|k) + E_{d\tau} d(i-\tau|k) \right), \quad i \in \{k, \dots, k+N_p-1\}, \tag{15d}$$

$$\underline{y} - \alpha(i|k) \le y(i|k) \le \overline{y} + \alpha(i|k), \quad i \in \{k, \dots, k+N_p-1\}, \tag{15e}$$

$$\underline{u}^g \le u^g(i+1|k) \le \overline{u}^g, \quad i \in \{k, \dots, k+N_p-1\}, \tag{15f}$$

$$\underline{u}^p \le u^p(i+1|k) \le \overline{u}^p, \quad i \in \{k, \dots, k+N_p-1\}, \tag{15g}$$

$$\underline{d}^{lo} \le d^{lo}(i+1|k) \le \overline{d}^{lo}, \quad i \in \{k, \dots, k+N_p-1\}, \tag{15h}$$

$$x(j|k) = \hat{x}_{MHE}(j|k), \quad j \in \{k-\tau, \dots, k-1\}, \tag{15i}$$

$$d^{lo}(l|k) = d^{lo}_{MPC}(l|k), \quad l \in \{k-\tau, \dots, k-1\}, \tag{15j}$$

$$u^g(l|k) = u^g_{MPC}(l|k), \quad l \in \{k-\tau, \dots, k-1\}, \tag{15k}$$

$$u^p(l|k) = u^p_{MPC}(l|k), \quad l \in \{k-\tau, \dots, k-1\}, \tag{15l}$$

where $\underline{y}, \overline{y}, \underline{u}^g, \overline{u}^g, \underline{u}^p$ and $\overline{u}^p$ denote the LNL, HNL, and lower and upper bounds on the gate and pumping control actions, respectively, and S_r is a selector matrix that enables to choose the suitable output subject to the delayed control. Moreover, $\underline{d}^{lo}$ and $\overline{d}^{lo}$ define the minimum and maximum number of allowed lock operations for those locks equipped with a turbine. Furthermore, $i \in \mathbb{Z}_{\ge 0}$ indicates the time instant along the prediction horizon, $k \in \mathbb{Z}_{\ge 0}$ denotes the time instants, and $k+i|k$ represents the predicted value of the variable at time $k+i$ by applying information known at time k, and $l \in \mathbb{Z}_{\ge 0}$ and $j \in \mathbb{Z}_{\ge 0}$ denote the use of information calculated in previous MHE or MPC iterations, for which the time intervals do not match the one indicated by i.

Then, solving (15) yields the optimal sequences $\mathbf{u}^{p*}(k) = \{u^p(i|k)\}_{i \in \mathbb{Z}_{[k,k+N_p-1]}}$, $\mathbf{u}^{g*}(k) = \{u^g(i|k)\}_{i \in \mathbb{Z}_{[k,k+N_p-1]}}$, $\mathbf{y}^*(k) = \{y(i|k)\}_{i \in \mathbb{Z}_{[k,k+N_p-1]}}$, $\alpha^*(k) = \{\alpha(i|k)\}_{i \in \mathbb{Z}_{[k,k+N_p-1]}}$ and $\mathbf{d}^{lo*}(k) = \left\{d^{lo}(i|k)\right\}_{i \in \mathbb{Z}_{[k,k+N_p-1]}}$. Taking into account the receding horizon philosophy, only the first values $u^{p*}(k|k)$ and $u^{g*}(k|k)$ from the optimal control

sequences $\mathbf{u}^{p*}(k)$ and $\mathbf{u}^{g*}(k)$ are considered, respectively, and $u^{p*}(k|k)$ is provided to the lower layer.

As a final remark, the high-tide MPC is equivalent to (15), except for the fact that $u^g(i|k)$ and $u^g(i-\tau_r|k)$ must be removed, as the gates cannot be used.

4.1.2. MHE formulation

Frequently, the system states are not completely available for measurement, and hence they must be estimated using an observer and available data. The MHE is used for this purpose, as it can provide this information. The underlying rationale involves expressing the estimation problem as a quadratic program, use a moving estimation window of constant size to consider a certain input–output data interval, and reconstruct the states for that time interval (Rao, Rawlings, & Lee, 2001). Indeed, only part of the available information is considered, which is shifted in time to estimate the states in a gradual manner.

Therefore, an MHE that estimates the states $\hat{x}_{MHE}$ and provides them to the MPC (15) can be designed as follows:

$$\min_{\hat{\mathbf{x}}_k} W^\top(k-N_e+1|k)P^{-1}W(k-N_e+1|k) + \sum_{i=k-N_e+1}^{k}\Big(W^\top(i|k)Q^{-1}W(i|k)+V^\top(i|k)R^{-1}V(i|k)\Big), \tag{16a}$$

subject to:

$$W(k-N_e+1|k)=\hat{x}(k-N_e+1|k)-x(k-N_e+1), \tag{16b}$$

$$W(i|k)=\hat{x}(i+1|k)-\Big(Ax(i|k)+B_u^g u^g(i|k)+B_u^p u^p(i|k) + B_d d(i|k)+\sum_{r=1}^{N_r}S_r\Big(B_{u\tau}^g u^g(i-\tau_r|k) + B_{u\tau}^p u^p(i-\tau_r|k)+B_{d\tau}d(i-\tau_r|k)\Big)\Big), \quad i\in\{k-N_e+1,\dots,k\} \tag{16c}$$

$$V(i|k)=y(i|k)-\Big(Cx(i|k)+D_u^g u^g(i|k)+D_u^p u^p(i|k) + D_d d(i|k)+\sum_{r=1}^{N_r}S_r\Big(D_{u\tau}^g u^g(i-\tau_r|k) + D_{u\tau}^p u^p(i-\tau_r|k)+D_{d\tau}d(i-\tau_r|k)\Big)\Big), \quad i\in\{k-N_e+1,\dots,k\} \tag{16d}$$

$$0=E_u^g u^g(i|k)+E_u^p u^p(i|k)+E_d d(i|k) + \sum_{\tau_i\in S}\left(E_{u\tau}^g u^g(i-\tau|k)+E_{u\tau}^p u^p(i-\tau|k)+E_{d\tau}d(i-\tau|k)\right), \quad i\in\{k-N_e+1,\dots,k\}, \tag{16e}$$

$$y(i|k)=y(i), \qquad i\in\{k-N_e+1,\dots,k\}, \tag{16f}$$

$$\underline{x}\le\hat{x}(i|k)\le\overline{x}, \qquad i\in\{k-N_e+1,\dots,k+1\}, \tag{16g}$$

$$\underline{d}^{lo}\le d^{lo}(i+1|k)\le\overline{d}^{lo}, \qquad i\in\{k-N_e-\tau+1,\dots,k\}, \tag{16h}$$

$$x(j|k)=\hat{x}_{MHE}(j|k), \qquad j\in\{k-N_e-\tau+1,\dots,k-N_e\}, \tag{16i}$$

$$d^{lo}(m|k)=d^{lo}_{MPC}(m|k), \qquad m\in\{k-N_e-\tau+1,\dots,k-N_e\}, \tag{16j}$$

$$u^g(m|k)=u^g_{MPC}(m|k), \qquad m\in\{k-N_e-\tau+1,\dots,k-N_e\}, \tag{16k}$$

$$u^p(m|k)=u^p_{MPC}(m|k), \qquad m\in\{k-N_e-\tau+1,\dots,k-N_e\}, \tag{16l}$$

where N_e is the estimation window size, and R^{-1} and Q^{-1} denote inverses of the weighting matrices of appropriate dimensions, which are defined in connection with the confidence in the measurements and model quality, respectively. The value $x(k-N_e+1)$ in (16a) represents the most likely initial state, $\hat{x}(k-N_e+1|k)$ corresponds to the first value of the sequence estimated by the MHE at time instant k, and $y(i)$ are the measured water levels. The initial estimate error, denoted with $\hat{x}(k-N_e+1|k)-x(k-N_e+1)$, is weighted by matrix P^{-1}, indicating the confidence into the initial state. The tuning of P^{-1} allows to guarantee estimation boundedness (Copp & Hespanha, 2017).

The least-squares problem is solved, and the optimal sequence $\hat{\mathbf{x}}^*(k)=\{\hat{x}(i|k)\}_{i\in\mathbb{Z}_{[k-N_e,k+1]}}$ is determined. However, as is the case when solving (15), a single value in the sequence is retained, which in this case is the last component, i.e. $\hat{x}(k+1|k)$.

4.2. Lower layer

The problem to be solved at this layer is that of determining the real control actions that can be applied to the actual system with the available equipment. These should be as close to the optimal control references (computed at the intermediate layer) as possible. Since it is assumed that gates can supply the exact flow, this task only needs to be done for the pumps.

More specifically, the main goal is to obtain the subset of pumps that should be activated at each time instant, such that the error between the optimal control reference and the applied control is minimal. This can be achieved by solving the following scheduling problem for every pumping station:

$$\min_{s_k^j} \quad \gamma_1\left\|T_{s_1}u^{p_j}_{MPC}(k)-T_{s_2}\sum_{i=k}^{k+G-1}\sum_{l=1}^{n_{p_j}}u_d^{p_j}(l)s_i^j(l)\right\|_2+\gamma_2(\Delta s_i^j)^\top(\Delta s_i^j), \tag{17a}$$

subject to:

$$s_i^j(l+1)+\Big(1-s_i^j(l)\Big)\le 1, \quad i\in\{k,\dots,k+G-1\}, \quad l\in\{1,\dots,n_{p_j}-1\}, \tag{17b}$$

$$s_i^j(l)\in\{0,1\}, \qquad i\in\{k,\dots,k+G-1\}, \quad l\in\{1,\dots,n_{p_j}\}, \tag{17c}$$

where j identifies the pumping station, i denotes the time instant, l indexes the position of the pump within the pumping station, and s_i^j is the vector of activation states of the pumps in the jth pumping station at the ith time instant. Moreover, n_{p_j} represents the number of pumps at the jth pumping station, $u_d^{p_j}(l)$ is the design flow of the lth pump at the jth pumping station, and $u^{p_j}_{MPC}(k)$ is the jth element of the optimal pumping action determined by the MPC. Furthermore, T_{s_1} and T_{s_2} are the sampling time of the upper and lower layers, respectively, and $G=T_{s_1}/T_{s_2}$ represents the total number of pumping actions within two successive MPC solutions. Finally, γ_1 and γ_2 are the weighting coefficients that define the relative importance of the objectives.

It must be noted that $s_i^j(l)=0$ indicates that the lth pump at the jth station is turned off at the ith time instant, and vice versa. A secondary objective is introduced in the cost function, as it is not desirable that the solution of (17) requires frequent changes in the activation states of the pumps. Moreover, the first constraint ensures sequential activation of the pumps.

The proposed two-layer approach assumes that the lower layer works with a faster sampling rate than the upper layer, i.e., $T_{s_1}>T_{s_2}$, which are selected so that $\mathrm{mod}(T_{s_1},T_{s_2})=0$. The simulation loop is executed using T_{s_2}, and therefore the corresponding MPC is solved once every G simulation time instants. The scheduling problem determines the next G real pumping actions, which are sequentially applied to the system (together with the optimal gate action). After that, the MHE is solved to determine the next state estimate, which allows to solve the next MPC. The multi-layer architecture is schematized in Fig. 1, which summarizes the main tasks carried out at each layer, as well as the interactions among layers and the system.

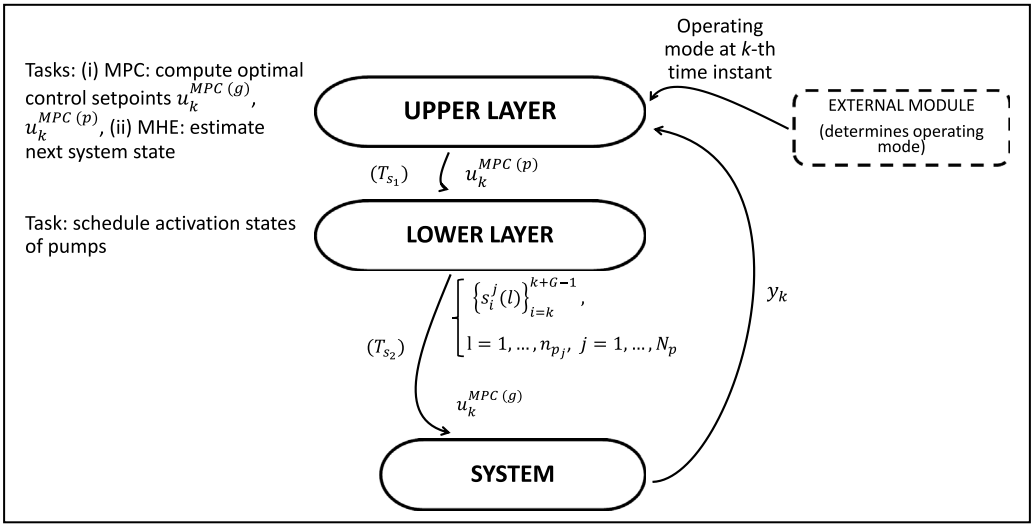

Fig. 1. Schematic representation of the multi-layer architecture.

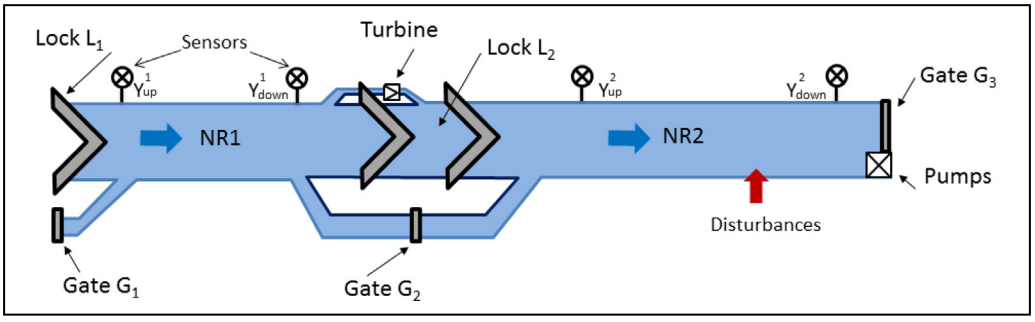

Fig. 2. Schematic representation of the considered system. (For interpretation of the references to colour in this figure legend, the reader is referred to the web version of this article.)

5. Application

5.1. Case study

The performance of the proposed approach is assessed using a case study based on a realistic system comprising two navigation reaches, NR_1 and NR_2, connected by a lock. These two canals are part of the inland waterways in the polder region in northern France. Polder regions are marine zones below sea level where water is collected using ditches. Water overflows in polders are pumped to navigation waterways and conveyed to the sea afterwards.

It should be noted that the Saint-Venant partial differential equations are used to model these two canals using the hydraulic software SIC[2] (Simulation and Integration of Control for Canals[1]) (Malaterre & Baume, 1997) Using a numerical discretization method, this software generates an accurate model of canals based on the solution of the Saint-Venant equations. Indeed, SIC[2] has been and still is extensively used by hydrographical network managers and hydraulic and control engineers to test and validate approaches prior to their implementation on the real system (Akhenak, Duviella, Bako, & Lecoeuche, 2013; Álvarez, Ridao, Ramirez, & Sánchez, 2013; Duviella, Chiron, & Charbonnaud, 2011; Horváth, Galvis, Gómez, & Rodellar, 2015b; Litrico, Fromion, Baume, Arranja, & Rijo, 2005; Lozano, Arranja, Rijo, & Mateos, 2010; Luppi, Malaterre, Battilani, Di Federico, & Toscano, 2018; Oubanas, Gejadze, Malaterre, & Mercier, 2018). Following this approach, and since access to the real system is not feasible, the effect of real disturbances on a model built in SIC[2] is studied. Moreover, a semidiurnal tidal pattern (two low and two high tides per day, each with an approximate duration of six hours) is considered given the canal location, as a historical record of the sea level is not available in this work.

Fig. 2 depicts a schematic view of the two-reach case study. Moreover, the physical data of each reach are presented in Table 1, where W and L are the bottom width and length, respectively, n_r is Manning's roughness coefficient, m_r represents the side slope (0 for a rectangular cross-section), s_b indexes the bottom slope (0 for a flat reach) and Q_s is the operating point used in the linearization of the Saint-Venant equations. Note that NR_1 is delimited by the locks L_1 and L_2, which are located at the upstream and downstream ends of the reach. At the same time, lock L_2 constitutes the upstream end of NR_2, while it is bounded at the downstream end by a pumping station (PS) consisting of four pumps (two with a design flow equal to 3 m^3/s, and another two with 2 m^3/s), and the sea outlet gate G_3. In addition to PS and G_3, the levels are regulated using two supplementary gates, G_1 and G_2. Note that the only gate whose use is restricted to low tide is G_3, while the other two may be employed regardless of the tidal period. Finally, and even though a turbine could be installed in every lock, only one is set up inside L_2 in this work. On the other hand, water level sensors are placed at the ends of both canals, and provide level measurements to the controllers.

The operational goals have different relative priorities for each canal. Indeed, in the case of NR_1, the control effort is directed towards keeping the level as close to the NNL as possible. Despite this is also desirable for NR_2, the focus is shifted towards maximizing energy production and minimizing the use of pumps for economic reasons and increase their useful life. For this purpose, the excess of water in the

[1] http://sic.g-eau.net.

Table 1
Characteristics of the studied system.

Reach	HNL [m]	NNL [m]	LNL [m]	L [m]	W [m]	n_r [s/m$^{1/3}$]	m_r [m/m]	s_b [m/m]	Q_s [m^3/s]
NR_1	3.95	3.8	3.65	42 000	50	0.035	0	0	0.6
NR_2	2.35	2.2	2.05	26 720	20	0.035	0	0	1

canal during high tide will be predicted, and thus the level will be lowered as much as possible during low tide. In this way, as much water as possible will be stored during high tide, so that its excess can be released into the sea at the next low tide using G_3, thus avoiding the use of pumps. It must be noted that it might still be necessary to operate the pumps during low tide, but this situation should only arise when G_3 has achieved its maximum capacity and there is still an excess of water in NR_2 that needs to be dispatched. On the other hand, and in order to maximize hydroelectricity production in NR_2, the number of lock operations performed by L_2, i.e., d_2, should be maximized. Indeed, hydroelectricity is generated via lock filling and draining operations, whereby the water flow induces rotation of the blades. It is important to note that, while d_2 is considered as a decision variable optimized through the solution of the MPC (to maximize energy generation), the operation of L_1, i.e., d_1, is assumed known. Finally, d_3, which is shown as disturbances in Fig. 2 (red arrow), is linked to the (uncontrolled) actions performed by farmers to eliminate the excess water due to the rain that is collected in the polder. Indeed, d_3 is considered under rainy conditions only in the second reach, and the waterways manager can expect d_3 to be present in rainy situations.

The linear discrete-time difference-algebraic equations with multiple delays (8) are considered in both MPC and MHE. Different time delays characterize each reach: two and a half hours for NR_1 and two hours for NR_2. For model discretization, sampling times $T_{s_1} = 20$ min and $T_{s_2} = 5$ min have been used, which are reasonable given the slow system dynamics. Moreover, both prediction horizon N_p and estimation window size N_e are considered equivalent to twelve hours to account for one complete high and low tide periods, as each has an average duration equal to 6 h. Furthermore, the flow supplied by the gates is bounded between 0 and 10 m^3/s. The weights of the cost function (12) for low tide and high tide are different for each scenario, which are described below. Indeed, the costs in the MPC can be adjusted to assign more priority to the most important objectives, and have been established by reiterative tuning until the appropriate performance is obtained. Their tuning is determined by minimizing the most important objective first while simultaneously maintaining suitable water levels inside the navigation rectangle, guaranteeing control action smoothness, penalizing relaxation parameter and maximizing energy generation.

Finally, simulation of the real conditions on the system built in SIC[2] allows to obtain results for a 24-hour period using the Gurobi 9.2 optimization package,[2] Matlab R2016b (64 bits) and YALMIP (Löfberg, 2004). These software tools are executed in a PC equipped with an Intel(R) Core i7-5500 CPU at 2.4 GHz with 12 GB of RAM.

5.2. Simulation results and discussion

In order to assess and analyse the proposed approach, the following three different scenarios are considered.

- Scenario I: the most important operational goal is to preserve the water level of each reach as close to the NNL as possible. According to this choice, the resulting lock operation profile for d_2, which is linked to hydroelectricity generation, is analysed. Moreover, the third lock operation profile, i.e., d_3, is assumed to be constant and equal to zero, which means that rain is not considered. The weights of the cost function (14) for low tide are set as follows: $W_y^{low} = 50$, $W_{ep}^{low} = 0.1$, $W_e^{low} = 10$, $W_{\Delta u}^{low} = 5$, and $W_\alpha^{low} = 1$. On the other hand, the high tide weights are: $W_y^{high} = 100$, $W_{ep}^{high} = 0.1$, $W_e^{high} = 10$, $W_{\Delta u}^{high} = 10$, and $W_\alpha^{high} = 1$.
- Scenario II: the operational goal with the highest priority is that of maximizing hydroelectricity production. Therefore, a lower relative priority is assigned to level setpoint tracking. This allows the levels to oscillate more around the NNL while keeping them within the [LNL, HNL] interval. Moreover, d_3 is also assumed equal to zero. In this scenario, and based on the priorities of the objectives, the weights are modified as follows: $W_y^{low} = 20$, $W_{ep}^{low} = 0.1$, $W_e^{low} = 10$, $W_{\Delta u}^{low} = 5$, and $W_\alpha^{low} = 1$. On the other hand, the high tide weights are: $W_y^{high} = 50$, $W_{ep}^{high} = 0.1$, $W_e^{high} = 10$, $W_{\Delta u}^{high} = 10$, and $W_\alpha^{high} = 1$.
- Scenario III: the same relative priorities as in the second scenario are considered. However, the effect of rain is analysed. Indeed, d_3 is considered as a known and measurable disturbance. Then, the result of maximizing d_2 is investigated. The weights used for both tidal periods are as in the second scenario.

The results and analysis of each of the above-mentioned scenarios using the proposed approach are jointly presented and compared. The optimal control actions, computed at the upper layer by the MPC for the different scenarios, are depicted in Fig. 3. It can be noted how the initial levels are below the NNL, and thus G_1 should open to fill the canal, whereas G_2 must remain closed so as to reach the NNL. The most remarkable result is related to G_3, which is shown in more detail in Fig. 4. The use of pumps is barely necessary during neither low nor high tide periods (even if gates cannot be used during the latter for safety reasons), thus complying with the minimization of economic pumping costs. The optimal pumping actions determined by the MPC are displayed in the top subplot of Fig. 4.

These optimal pumping actions are then sent to the lower layer as input to the scheduling problem. It is considered that each pump may be activated for any duration equal to $\{0, 5, 10, 15, 20\}$ minutes between two consecutive MPC solutions. It can be seen in Fig. 5 that the pumps are not activated in any scenario. Indeed, the scheduling problem is formulated bearing in mind real applications, in which it is not desirable to switch the activation states very frequently. Then, constant ON/OFF pump switching can be limited (or even avoided) by considering a large weight on the smoothness of real pumping actions. This is indeed the preferred system behaviour from the standpoint of the managers, who do not want to activate and deactivate the pumps too often due to associated maintenance problems. Instead, it is their preference to relax the control of the levels (as long as they are kept within the navigation rectangle), if this results in pumps being operated less frequently . Moreover, the optimal pumping values are already rather small to consider pumping, which is why the decision taken at the lower layer is that of keeping the pumps off at all times.

On the other hand, the water levels that result from applying the previous control signals are represented in Fig. 6. The results for the first scenario show that the level stays around the NNL for both canals, and inside the navigation ranges. On the other hand, the levels in NR_2 for the second and third scenarios are not as close to the NNL as for the first one due to the prioritization of objectives. Indeed, the level is allowed to oscillate around the NNL to maximize d_2 during the day. In fact, when the water levels are allowed to oscillate more, longer times might be needed to perform lock filling and draining operations, and thus maximize energy production. In order to allow for a quantitative performance assessment, the tracking errors between the water levels

[2] https://www.gurobi.com/.

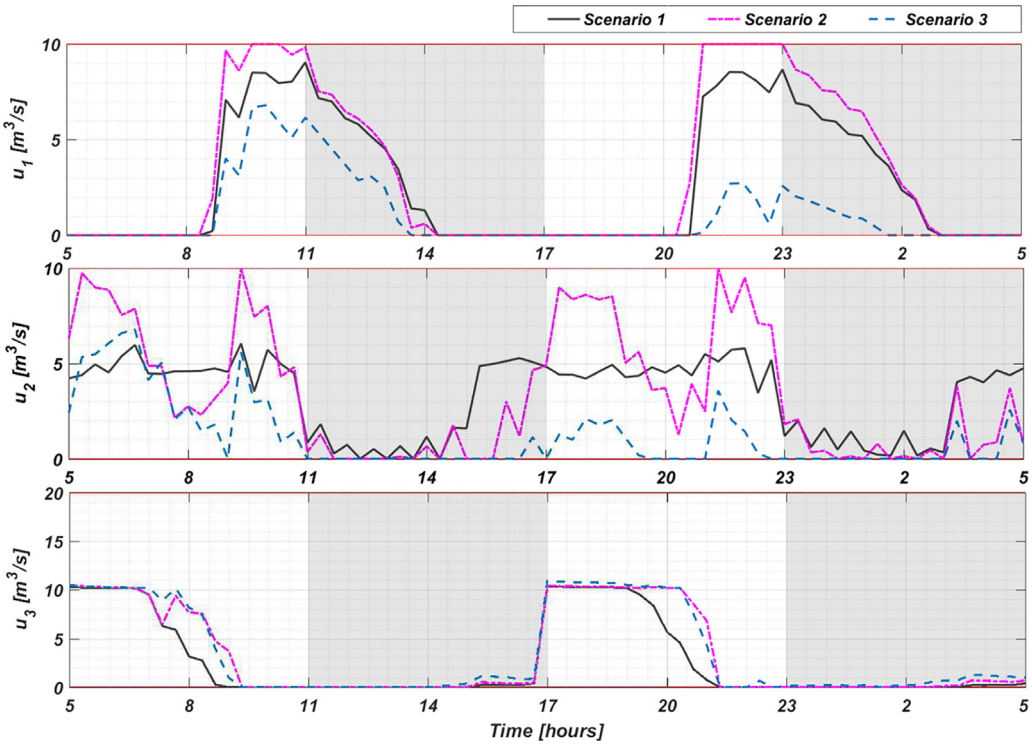

Fig. 3. Comparison of optimal control actions and bounds (solid red lines). (For interpretation of the references to colour in this figure legend, the reader is referred to the web version of this article.)

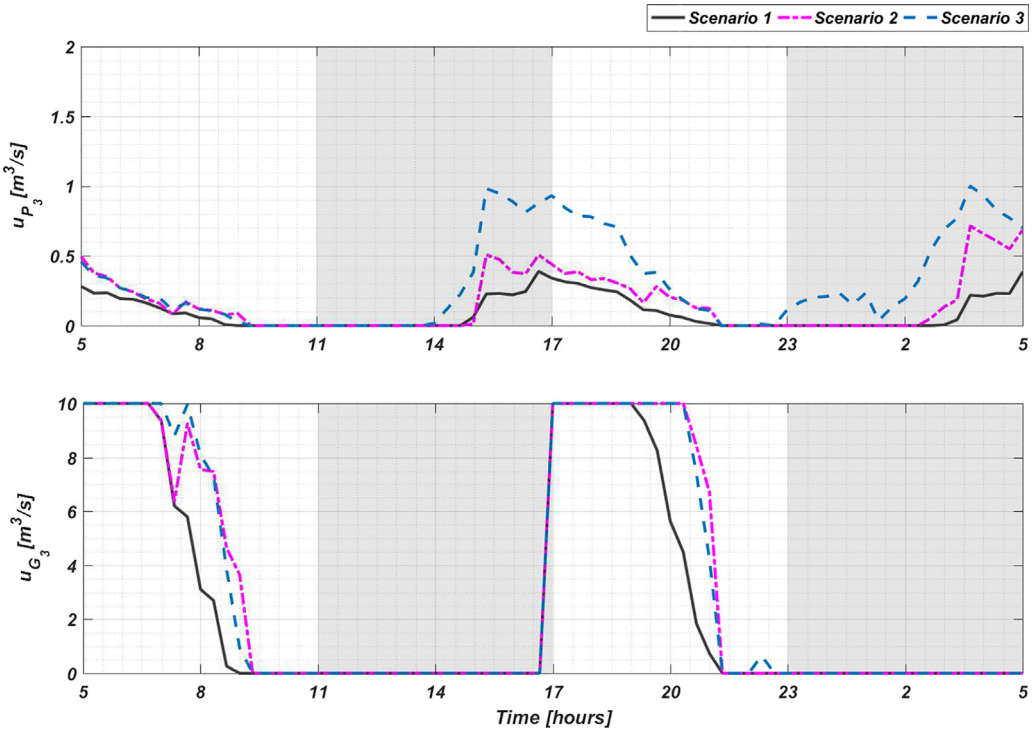

Fig. 4. Comparison of optimal pumping and gate actions at the downstream end of NR_2.

and setpoints are determined by means of the following indicators (Segovia et al., 2019):

$$TP = 1 - \frac{1}{N_p}\sqrt{\sum_{k=1}^{N_p}\left(\frac{y_k - y_{ref}}{\frac{1}{2}\left(\overline{y}_{ref} - \underline{y}_{ref}\right)}\right)^2}. \tag{18}$$

Table 2 summarizes the tracking performances (TP) for all scenarios, whereby the satisfactory performance of the control approach can be verified. Note that the tracking performance can take values between 0 and 1, where 1 means perfect tracking. It can then be observed that the tracking performance in the first scenario is better than in the other cases due to the priority given to this objective.

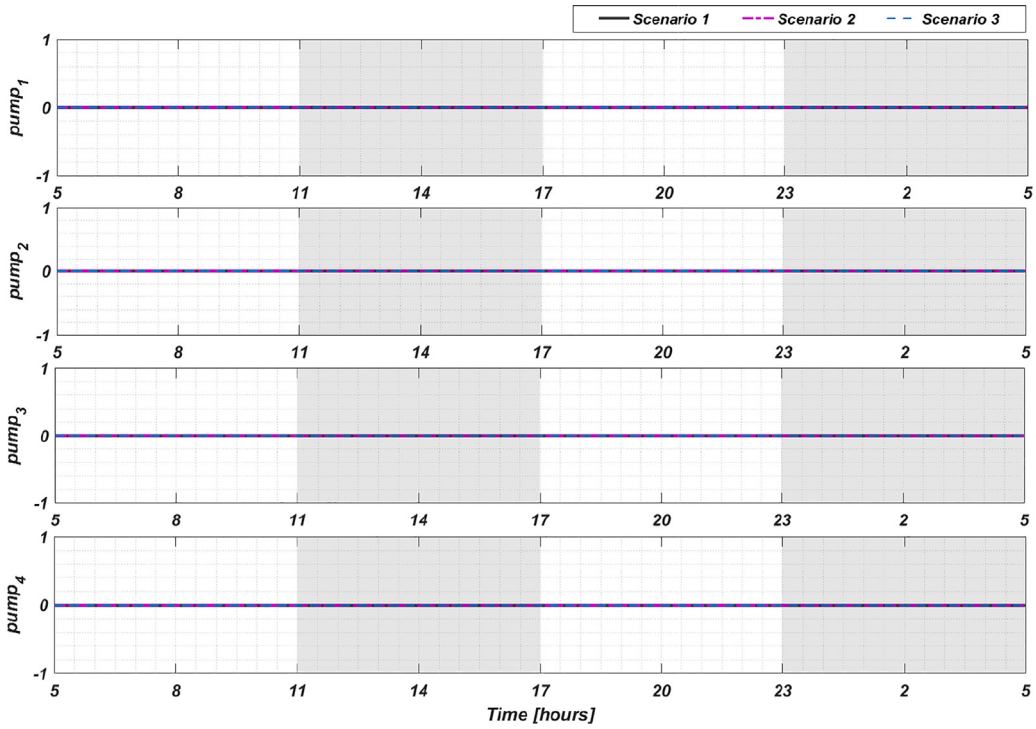

Fig. 5. Comparison of activation of pumps.

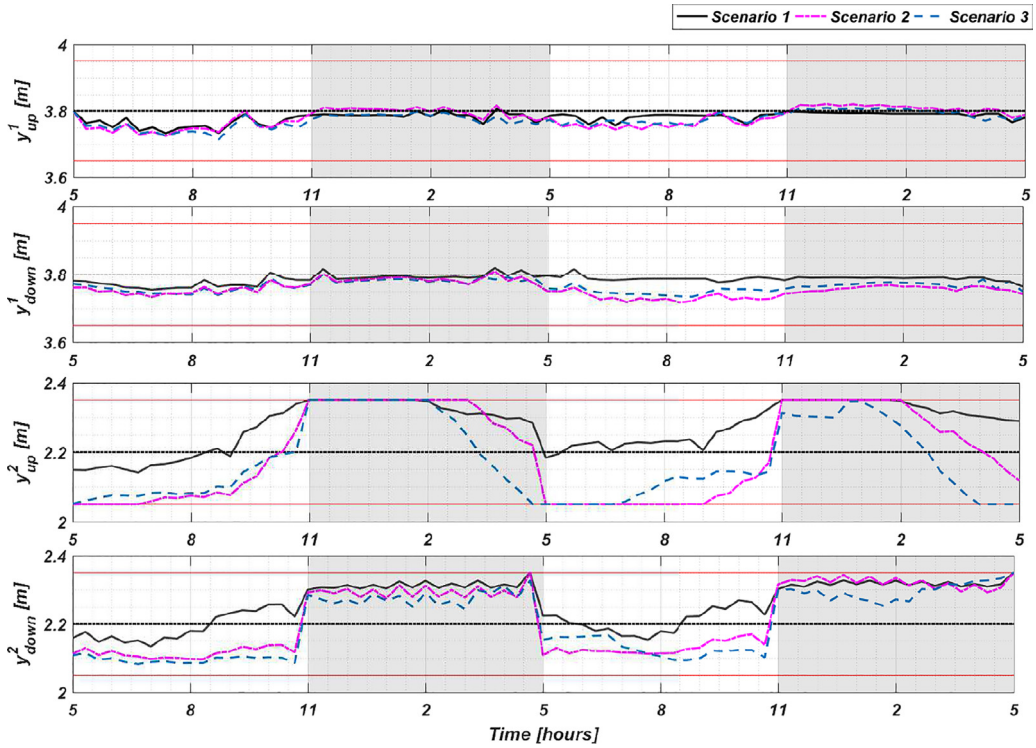

Fig. 6. Comparison of water levels, NNL (black dotted line), and HNL and LNL (red solid lines). (For interpretation of the references to colour in this figure legend, the reader is referred to the web version of this article.)

Then, the optimal gate actions and the scheduled pumping actions are implemented into the system (built in SIC^2), and the resulting water levels are determined. This information is stored and conveniently sent to the MHE, so that the states at the next time instant can be estimated. Figs. 7–9 depict the comparison between states computed utilizing the simplified model and the actual state estimates for the first, second and third scenarios, respectively. Moreover, key performance indicators associated to computation times are defined and obtained for each scenario. On the one hand, KPI_t is defined as the average time required to solve the two optimization problems (MPC + MHE) per time step. On the other hand, total simulation times are also provided. Therefore, the KPI_t for the first scenario is 4.5159 s, while the simulation time

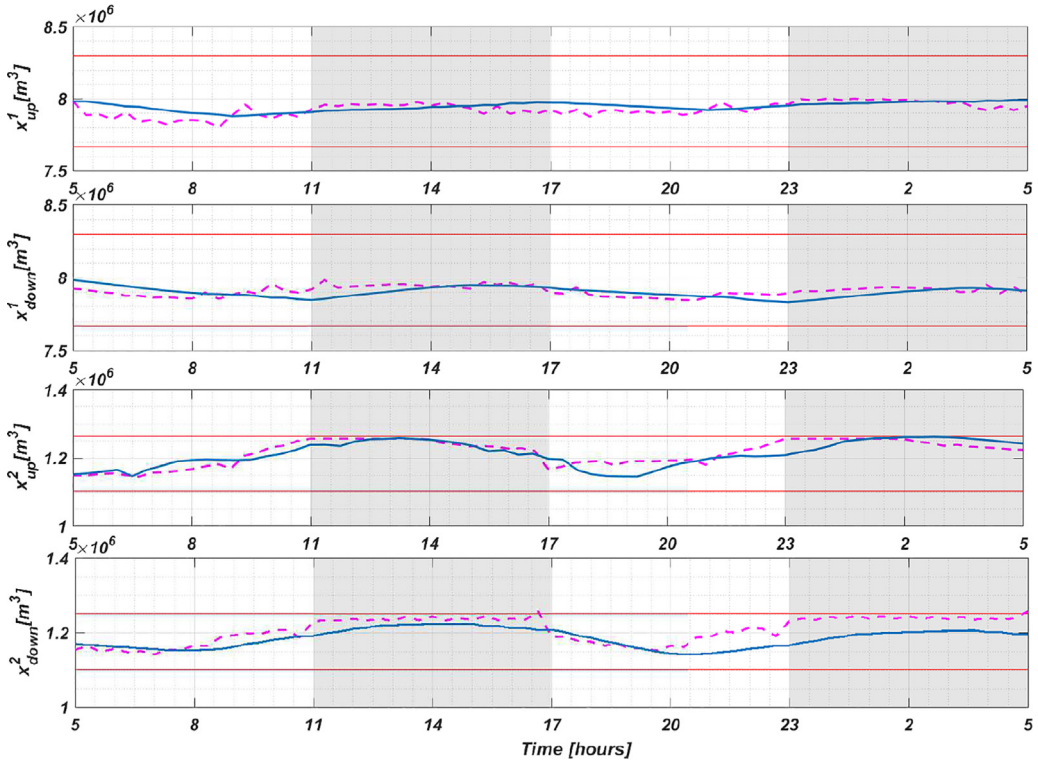

Fig. 7. State estimates (purple dash-dot lines) and computed states (blue solid lines) for Scenario I.

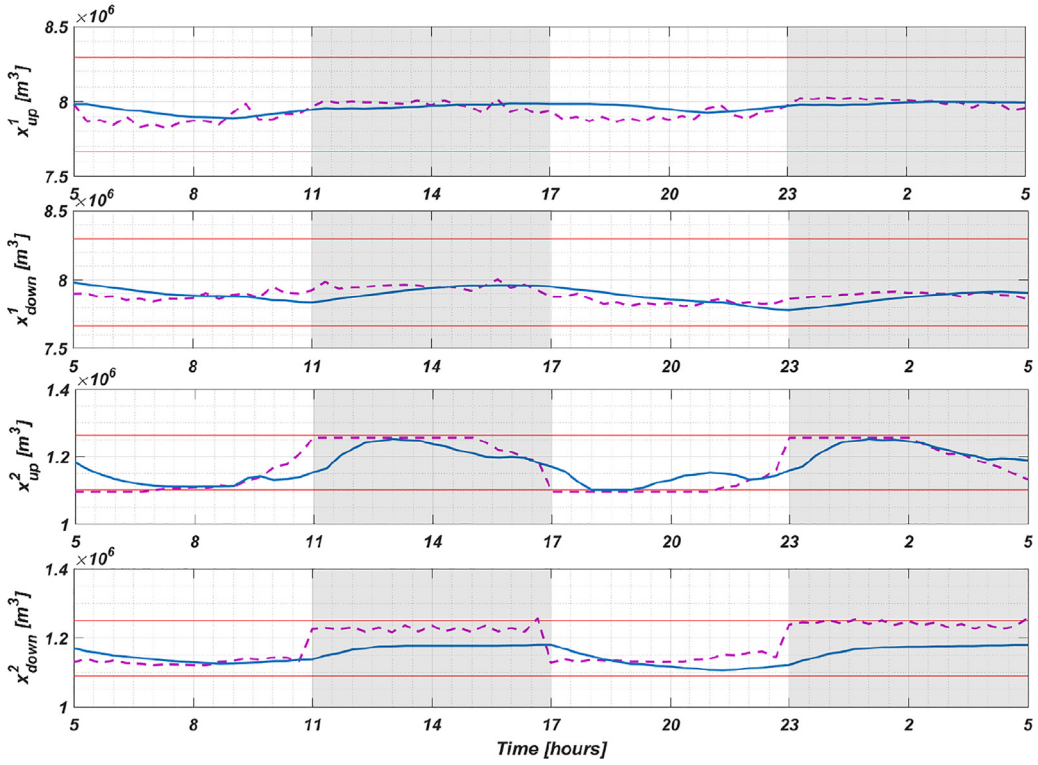

Fig. 8. State estimates (purple dash-dot lines) and computed states (blue solid lines) for Scenario II.

is 346.073 s. The KPI_t in the second scenario is 4.2630 s, with a simulation time of 323.956 s. Finally, in the third scenario, a KPI_t of 4.7407 s and a simulation time of 351.5600 s are obtained. It can therefore be concluded that these values are rather similar for all scenarios.

Finally, the lock operation profiles obtained for all scenarios are depicted in Fig. 10. As mentioned above, d_1 is assumed as a known measured disturbance in all scenarios, while the effect of d_3 is only considered in the third scenario, i.e., $d_3 = 0$ during the whole first and second scenarios. Therefore, energy production results are linked to d_2

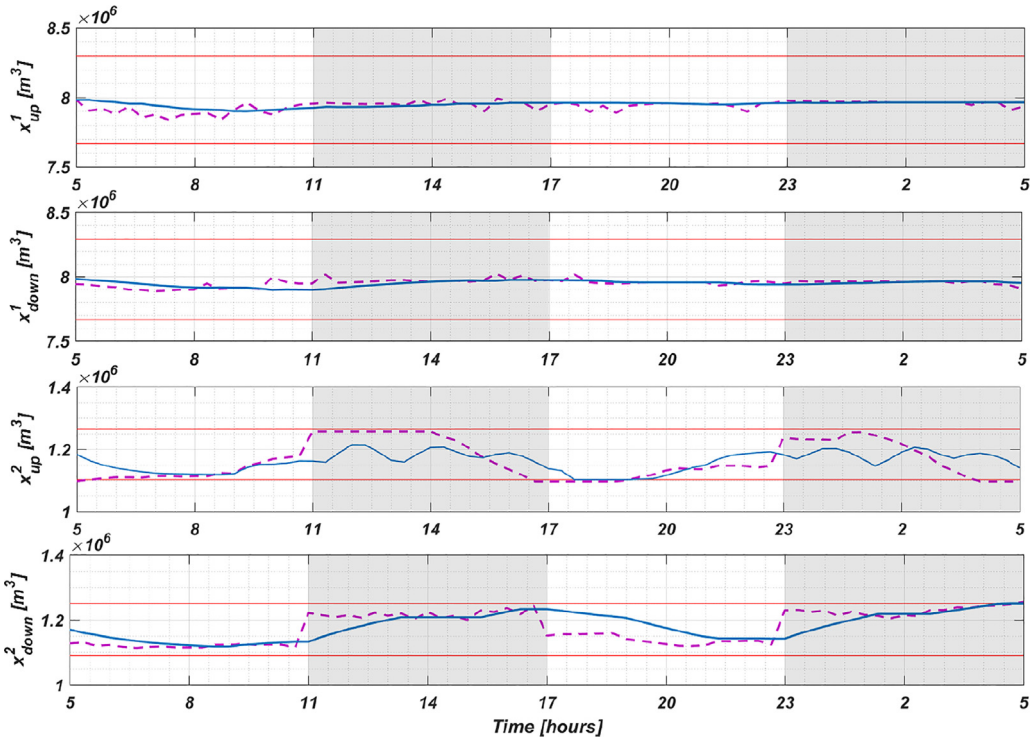

Fig. 9. State estimates (purple dash-dot lines) and computed states (blue solid lines) for Scenario III.

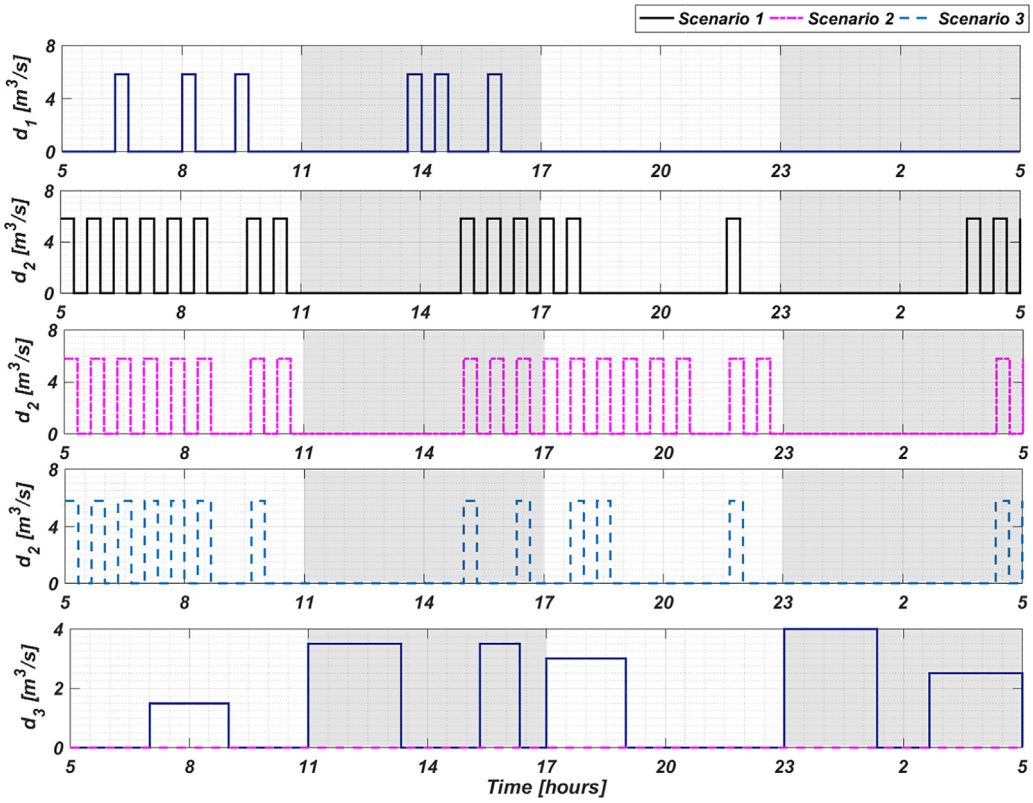

Fig. 10. Comparison of evolution of lock operations.

(lock L_2), which is a decision variable in the MPC formulation, as the turbine is located in this lock. Table 3 presents the numeric evaluation of the above scenarios for energy production and the number of lock operations. Note that each lock operation generates 6.21 MJ (Leontidis et al., 2016). According to Fig. 10, and analysing the results in Table 3, it can be discerned that the number of lock operations in the second scenario is higher than for other scenarios. Energy production is improved by 25% with respect to the first scenario while keeping a satisfactory tracking performance, which only decreases by 1.4% in the second reach. On the other hand, the third scenario has the lowest

Table 2
Comparison of tracking performances.

Reach	Scenario 1	Scenario 2	Scenario 3
NR_1	0.9797	0.9737	0.9733
NR_2	0.9433	0.9301	0.9258

Table 3
Comparison of the amount of energy produced.

Criteria	Scenario 1	Scenario 2	Scenario 3
Number of lock operations	16	20	13
Energy production (MJ)	99.36	124.2	80.73

amount of lock operations, which is due to the effect of d_3. Indeed, the disturbances considered in this scenario have a higher impact on the water levels, and thus complicate the issue of controlling the levels within bounds. Therefore, the second lock cannot be further operated to boost energy production. However, it can be realized that d_2 is increased to maximize energy production in all scenarios, while the levels are kept inside the navigation rectangle to avoid the impacts of severe weather events.

6. Conclusions

This paper focused on a combined hierarchical control and state estimation approach for maximizing hydroelectricity generation while ensuring the navigability of inland waterways. To this end, a two-layer control strategy was designed, each of them tasked with part of the overall problem. The issue of hydroelectricity generation was tackled using a turbine inside of a lock, and its maximization was achieved by maximizing the number of lock operations such that the water levels never exceeded the navigation interval. The proposed strategy was applied on a model of part of the inland waterways in northern France, which was built using a specific hydraulic software tool. The simulation results allowed to demonstrate the effectiveness of the methodology, and showed that the number of lock operations can effectively be increased to maximize energy production while maintaining the water levels inside the navigation interval, thus keeping the effects of severe weather episodes under control.

Future research regards the consideration of a more detailed mathematical model of the turbine, such as the one presented in Zhang et al. (2018). This model could be incorporated into the dynamic inland waterway model, and should result in improved accuracy and performance of the approach. Moreover, while this work assumes known disturbances, this is not always the case, especially for environmental systems. In this regard, it could be of interest to consider unknown input observers (UIO), which do not require previous knowledge about these inputs (Guan & Saif, 1991). Furthermore, it is assumed that the system works close to the same operating point throughout the entire simulation, a rather limited assumption in the case of large operating ranges. Then, the current model could be formulated in the linear-parameter varying (LPV) paradigm, making use of existing results for irrigation canals (Bolea, Puig, & Blesa, 2014). Finally, non-centralized control (Fele, Maestre, Hashemy, Muñoz de la Peña, & Camacho, 2014; Segovia, Puig, Duviella and Etienne, 2021; Zhang, Zheng, & Li, 2019) and state estimation (Rodriguez, Maestre, Camacho, & Sánchez, 2020; Segovia, Puig and Duviella, 2021) methodologies could be examined to improve reliability and scalability of the approach, as they have proven to be well suited to deal with large-scale systems.

Declaration of competing interest

The authors declare that they have no known competing financial interests or personal relationships that could have appeared to influence the work reported in this paper.

Acknowledgements

This work has been partially funded by the project CHEEF2 from the Regional Council Hauts-de-France. The support is gratefully acknowledged.

References

Ackermann, T., Schwanenberg, D., Natschke, M., Köngeter, J., Refsgaard, J., & Karalis, E. (1997). Control strategy for river-power-plants based on optimization. *Operational Water Management*, 285–288.

Akhenak, A., Duviella, E., Bako, L., & Lecoeuche, S. (2013). Online fault diagnosis using recursive subspace identification: Application to a dam-gallery open channel system. *Control Engineering Practice*, *21*(6), 797–806.

Álvarez, A., Ridao, M. A., Ramirez, D. R., & Sánchez, L. (2013). Constrained predictive control of an irrigation canal. *Journal of Irrigation and Drainage Engineering*, *139*(10), 841–854.

Bolea, Y., Puig, V., & Blesa, J. (2014). Linear parameter varying modeling and identification for real-time control of open-flow irrigation canals. *Environmental Modelling & Software*, *53*, 87–97.

Breckpot, M., Blanco, T. B., & De Moor, B. (2010). Flood control of rivers with nonlinear model predictive control and moving horizon estimation. In *49th IEEE conference on decision and control (CDC)* (pp. 6107–6112). IEEE.

Chow, V. (1959). Chapter 5. In *Open-channel hydraulics, vol. 1* (pp. 89–114). New York, NY, USA: McGraw-Hill Book Company.

Copp, D. A., & Hespanha, J. P. (2017). Simultaneous nonlinear model predictive control and state estimation. *Automatica*, *77*, 143–154.

Desy, N., & Virta, P. (2005). Ship lock electrical energy generation. US Patent 6, 969, 925.

Duviella, E., Chiron, P., & Charbonnaud, P. (2011). A reactive control strategy for networked hydrographical system management. *Control Engineering Practice*, *19*(8), 851–861.

Fele, F., Maestre, J. M., Hashemy, S. M., Muñoz de la Peña, D., & Camacho, E. F. (2014). Coalitional model predictive control of an irrigation canal. *Journal of Process Control*, *24*(4), 314–325.

Guan, Y., & Saif, M. (1991). A novel approach to the design of unknown input observers. *IEEE Transactions on Automatic Control*, *36*(5), 632–635.

Guekam, P., Segovia, P., Etienne, L., & Duviella, E. (2021). Hierarchical model predictive control and moving horizon estimation for open-channel systems with multiple time delays. In *2021 european control conference (ECC)* (pp. 198–203).

Horváth, K., Duviella, E., Blesa, J., Rajaoarisoa, L., Bolea, Y., Puig, V., et al. (2014). Gray-box model of inland navigation channel: application to the cuinchy–fontinettes reach. *Journal of Intelligent Systems*, *23*(2), 183–199.

Horváth, K., Galvis, E., Gómez, M., & Rodellar, J. (2015a). Is it better to use gate opening as control variable than discharge to control irrigation canals? *Journal of Irrigation and Drainage Engineering*, *141*(3), Article 04014054.

Horváth, K., Galvis, E., Gómez, M., & Rodellar, J. (2015b). New offset-free method for model predictive control of open channels. *Control Engineering Practice*, *41*, 13–25.

Joseph-Duran, B., Ocampo-Martinez, C., & Cembrano, G. (2015). Output-feedback control of combined sewer networks through receding horizon control with moving horizon estimation. *Water Resources Research*, *51*(10), 8129–8145.

Karimi Pour, F., Puig, V., & Cembrano, G. (2019a). Economic health-aware LPV-mpc based on system reliability assessment for water transport network. *Energies*, *12*(15), 3015.

Karimi Pour, F., Puig, V., & Cembrano, G. (2019b). Economic MPC-LPV control for the operational management of water distribution networks. *IFAC-PapersOnLine*, *52*(23), 88–93.

Karimi Pour, F., Puig, V., & Cembrano, G. (2020). Economic reliability-aware MPC-lpv for operational management of flow-based water networks including chance-constraints programming. *Processes*, *8*(1), 60.

Karimi Pour, F., Puig, V., & Ocampo-Martinez, C. (2017). Economic predictive control of a pasteurization plant using a linear parameter varying model. In *Computer aided chemical engineering, vol. 40* (pp. 1573–1578). Elsevier.

Karimi Pour, F., Puig, V., & Ocampo-Martinez, C. (2019). Model predictive control based on LPV models with parameter-varying delays. In *2019 18th european control conference (ECC)* (pp. 3644–3649). IEEE.

Karimi Pour, F., Puig, V., & Ocampo-Martinez, C. (2021). Economic model predictive control of nonlinear systems using a linear parameter varying approach. *International Journal of Robust and Nonlinear Control*.

Kraus, T., Ferreau, H. J., Kayacan, E., Ramon, H., De Baerdemaeker, J., Diehl, M., et al. (2013). Moving horizon estimation and nonlinear model predictive control for autonomous agricultural vehicles. *Computers and Electronics in Agriculture*, *98*, 25–33.

Lao, L., Ellis, M., Durand, H., & Christofides, P. D. (2015). Real-time preventive sensor maintenance using robust moving horizon estimation and economic model predictive control. *AIChE Journal*, *61*(10), 3374–3389.

Leontidis, V., Zhang, J., Caignaert, G., Delarue, P., Tounzi, A., Piriou, F., et al. (2016). Lock hydro-electrical power generation feasability study.

Litrico, X., & Fromion, V. (2009). *Modeling and control of hydrosystems*. Springer Science & Business Media.

Litrico, X., Fromion, V., Baume, J. P., Arranja, C., & Rijo, M. (2005). Experimental validation of a methodology to control irrigation canals based on saint-venant equations. *Control Engineering Practice*, *13*(11), 1425–1437.

Litrico, X., Malaterre, P. O., Baume, J. P., & Ribot-Bruno, J. (2008). Conversion from discharge to gate opening for the control of irrigation canals. *Journal of Irrigation and Drainage Engineering*, *134*(3), 305–314.

Löfberg, J. (2004). YALMIP: a toolbox for modeling and optimization in MATLAB. In *2004 IEEE international conference on robotics and automation* (pp. 284–289).

Lozano, D., Arranja, C., Rijo, M., & Mateos, L. (2010). Simulation of automatic control of an irrigation canal. *Agricultural Water Management*, *97*(1), 91–100.

Luppi, M., Malaterre, P. O., Battilani, A., Di Federico, V., & Toscano, A. (2018). A multi-disciplinary modelling approach for discharge reconstruction in irrigation canals: The canale emiliano romagnolo (northern Italy) case study. *Water*, *10*(8).

Maestre, J., Ridao, M., Kozma, A., Savorgnan, C., Diehl, M., Doan, M., et al. (2015). A comparison of distributed MPC schemes on a hydro-power plant benchmark. *Optimal Control Applications & Methods*, *36*(3), 306–332.

Malaterre, P. O., & Baume, J. P. (1997). SIC 3.0, a simulation model for canal automation design. In *International workshop on the regulation of irrigation canals, vol. 1* (pp. 68–75).

Nguyen, L., Prodan, I., Lefevre, L., & Genon-Catalot, D. (2017). Distributed model predictive control of irrigation systems using cooperative controllers. *IFAC-PapersOnLine*, *50*(1), 6564–6569.

Oubanas, H., Gejadze, I., Malaterre, P. O., & Mercier, F. (2018). River discharge estimation from synthetic SWOT-type observations using variational data assimilation and the full saint-venant hydraulic model. *Journal of Hydrology*, *559*, 638–647.

Puig, V., Ocampo-Martínez, C., & Negenborn, R. (2015). Model predictive control for combined water supply and navigability/sustainability in river systems. In *Transport of water versus transport over water* (pp. 13–33). Springer.

Quintero, S. A., Copp, D. A., & Hespanha, J. P. (2015). Robust UAV coordination for target tracking using output-feedback model predictive control with moving horizon estimation. In *2015 american control conference (ACC)* (pp. 3758–3764). IEEE.

Rajaoarisoa, L., Horvath, K., Duviella, E., & Chuquet, K. (2014). Large-scale system control based on decentralized design. Application to cuinchy fontinette reach. *IFAC Proceedings Volumes*, *47*(3), 11105–11110.

Rao, C. V., Rawlings, J. B., & Lee, J. H. (2001). Constrained linear state estimation—a moving horizon approach. *Automatica*, *37*(10), 1619–1628.

Ribeiro, A., Guedes, M., Smirnov, G., & Vilela, S. (2012). On the optimal control of a cascade of hydro-electric power stations. *Electric Power Systems Research*, *88*, 121–129.

Rodriguez, L. P., Maestre, J. M., Camacho, E. F., & Sánchez, M. C. (2020). Decentralized ellipsoidal state estimation for linear model predictive control of an irrigation canal. *Journal of Hydroinformatics*, *22*(3), 593–605.

Şahin, A., & Morari, M. (2010). Decentralized model predictive control for a cascade of river power plants. In *Intelligent infrastructures* (pp. 463–485). Springer.

Schuurmans, J., Clemmens, A., Dijkstra, S., Hof, A., & Brouwer, R. (1999). Modeling of irrigation and drainage canals for controller design. *Journal of Irrigation and Drainage Engineering*, *125*(6), 338–344.

Segovia, P., Blesa, J., Horváth, K., Rajaoarisoa, L., Nejjari, F., Puig, V., et al. (2018). Modeling and fault diagnosis of flat inland navigation canals. *Proceedings of the Institution of Mechanical Engineers, Part I: Journal of Systems and Control Engineering*, *232*(6), 761–771.

Segovia, P., Duviella, E., & Puig, V. (2020). Multi-layer model predictive control of inland waterways with continuous and discrete actuators. *IFAC-PapersOnLine*, *53*(2), 16624–16629, 21th IFAC World Congress.

Segovia, P., Puig, V., & Duviella, E. (2021). Set-membership-based distributed moving horizon estimation of large-scale systems. *ISA Transactions*.

Segovia, P., Puig, V., Duviella, E., & Etienne, L. (2021). Distributed model predictive control using optimality condition decomposition and community detection. *Journal of Process Control*, *99*, 54–68.

Segovia, P., Rajaoarisoa, L., Nejjari, F., Duviella, E., & Puig, V. (2019). Model predictive control and moving horizon estimation for water level regulation in inland waterways. *Journal of Process Control*, *76*, 1–14.

Setz, C., Heinrich, A., Rostalski, P., Papafotiou, G., & Morari, M. (2008). Application of model predictive control to a cascade of river power plants. *IFAC Proceedings Volumes*, *41*(2), 11978–11983.

Van Overloop, P., Miltenburg, I., Bombois, X., Clemmens, A., Strand, R., Van De Giesen, N., et al. (2010). Identification of resonance waves in open water channels. *Control Engineering Practice*, *18*(8), 863–872.

Van Overloop, P., Negenborn, R., De Schutter, B., & Van De Giesen, N. (2010). Predictive control for national water flow optimization in The Netherlands. In *Intelligent infrastructures* (pp. 439–461). Springer.

Vukov, M., Gros, S., Horn, G., Frison, G., Geebelen, K., Jørgensen, J. B., et al. (2015). Real-time nonlinear MPC and MHE for a large-scale mechatronic application. *Control Engineering Practice*, *45*, 64–78.

Weyer, E. (2001). System identification of an open water channel. *Control Engineering Practice*, *9*(12), 1289–1299.

Yin, M., Li, W., Chung, C. Y., Zhou, L., Chen, Z., & Zou, Y. (2016). Optimal torque control based on effective tracking range for maximum power point tracking of wind turbines under varying wind conditions. *IET Renewable Power Generation*, *11*(4), 501–510.

Zhang, J., Leontidis, V., Dazin, A., Tounzi, A., Delarue, P., Caignaert, G., et al. (2018). Canal lock variable speed hydropower turbine design and control. *IET Renewable Power Generation*, *12*(14), 1698–1707.

Zhang, J., Tounzi, A., Delarue, P., Piriou, F., Leontidis, V., Dazin, A., et al. (2017). Canal lock variable speed hydropower turbine energy conversion system. In *2017 twelfth international conference on ecological vehicles and renewable energies (EVER)* (pp. 1–6). IEEE.

Zhang, Y., Zheng, Y., & Li, S. (2019). Enhancing cooperative distributed model predictive control for the water distribution networks pressure optimization. *Journal of Process Control*, *84*, 70–88.

Zhou, Z., Scuiller, F., Charpentier, J. F., Benbouzid, M. E. H., & Tang, T. (2013). Power smoothing control in a grid-connected marine current turbine system for compensating swell effect. *IEEE Transactions on Sustainable Energy*, *4*(3), 816–826.